Acta Crystallographica Section B
Structural Science
ISSN 0108-7681

Structure determination of seven phases and solvates of Pigment Yellow 183 and Pigment Yellow 191 from X-ray powder and single-crystal data

Svetlana N. Ivashevskaya,[a,b] Jacco van de Streek,[a,c] Juste E. Djanhan,[a] Jürgen Brüning,[a] Edith Alig,[a] Michael Bolte,[a] Martin U. Schmidt,[a]* Peter Blaschka,[d] Hans Wolfgang Höffken[d] and Peter Erk[d]

[a]Institute of Inorganic and Analytical Chemistry, Goethe University, Max-von-Laue-Strasse 7, D-60438 Frankfurt am Main, Germany, [b]Institute of Geology, Karelian Research Centre, Russian Academy of Sciences, Pushkinskaya 11, 185910 Petrozavodsk, Russia, [c]Avant-garde Materials Simulation, Merzhauserstrasse 177, D-79100 Freiburg, Germany, and [d]BASF SE, Research Specialty Chemicals, D-67056 Ludwigshafen, Germany

Correspondence e-mail: m.schmidt@chemie.uni-frankfurt.de

Received 16 September 2008
Accepted 14 January 2009

The crystal structures of two industrially produced laked yellow pigments, Pigment Yellow 183 [P.Y. 183, $Ca(C_{16}H_{10}Cl_2N_4O_7S_2)$, α phase] and Pigment Yellow 191 [P.Y. 191, $Ca(C_{17}H_{13}ClN_4O_7S_2)$, α and β phases], were determined from laboratory X-ray powder diffraction data. The coordinates of the molecular fragments of the crystal structures were found by means of real-space methods (simulated annealing) with the program *DASH*. The coordinates of the calcium ions and the water molecules were determined by combining real-space methods (*DASH* and *MRIA*) and repeated Rietveld refinements (*TOPAS*) of the partially finished crystal structures. *TOPAS* was also used for the final Rietveld refinements. The crystal structure of β-P.Y. 183 was determined from single-crystal data. The α phases of the two pigments are isostructural, whereas the β phases are not. All four phases exhibit a double-layer structure, built from nonpolar layers containing the C/N backbone and polar layers containing the calcium ions, sulfonate groups and water molecules. Furthermore, the crystal structures of an *N*,*N*-dimethylformamide solvate of P.Y. 183, and of P.Y. 191 solvates with *N*,*N*-dimethylformamide and *N*,*N*-dimethylacetamide were determined by single-crystal X-ray analysis.

1. Introduction

Pigments are practically insoluble in their application media; they are not dissolved, but finely dispersed. Hence their crystal structures are maintained and the properties of the final product depend on the solid-state structure of the pigments. This holds for inorganic as well as for organic pigments.

Pigment Yellow 183 (P.Y. 183) and Pigment Yellow 191 (P.Y. 191) are commercially important yellow pigments (P.Y. 183 is produced by *e.g.* BASF, whereas P.Y. 191 is produced by *e.g.* Clariant). Both compounds are calcium lakes of pyrazolone azo pigments; their structural formulae are shown in Fig. 1.

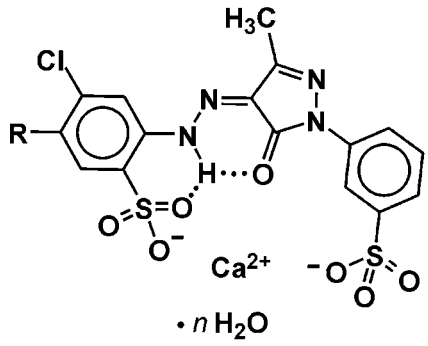

Figure 1
Chemical structures of P.Y. 183 (R = Cl) and P.Y. 191 (R = CH_3). n = 0–3, depending on the crystal phase.

P.Y. 183 and P.Y. 191 afford reddish-yellow shades. Owing to their excellent photostability they are mainly used for the colouration of plastics, especially for outdoor applications like plastic films in the agricultural field (*e.g.* yellow films for covering beds). P.Y. 191 is also used for hot-melting traffic paints in the USA.

For P.Y. 191 five phases (α, β, γ, δ and ε) are known (Schmidt *et al.*, 2002*a*). The α (Deucker, 1990) and β (Schmidt *et al.*, 2002*b*) phases are industrially produced. P.Y. 183 exists in at least four phases, which we denote as α, β, ζ and η (Schmidt, 2008). Phases α and β are produced commercially. The industrial synthesis of these azo pigments is shown in Fig. 2.

In the solid state all commercial 'azo' pigments actually do not contain an 'azo' group (—N=N—), but a hydrazone group (—NH—N=), as is known from single-crystal structure analysis and various spectroscopic investigations (Herbst & Hunger, 2004).

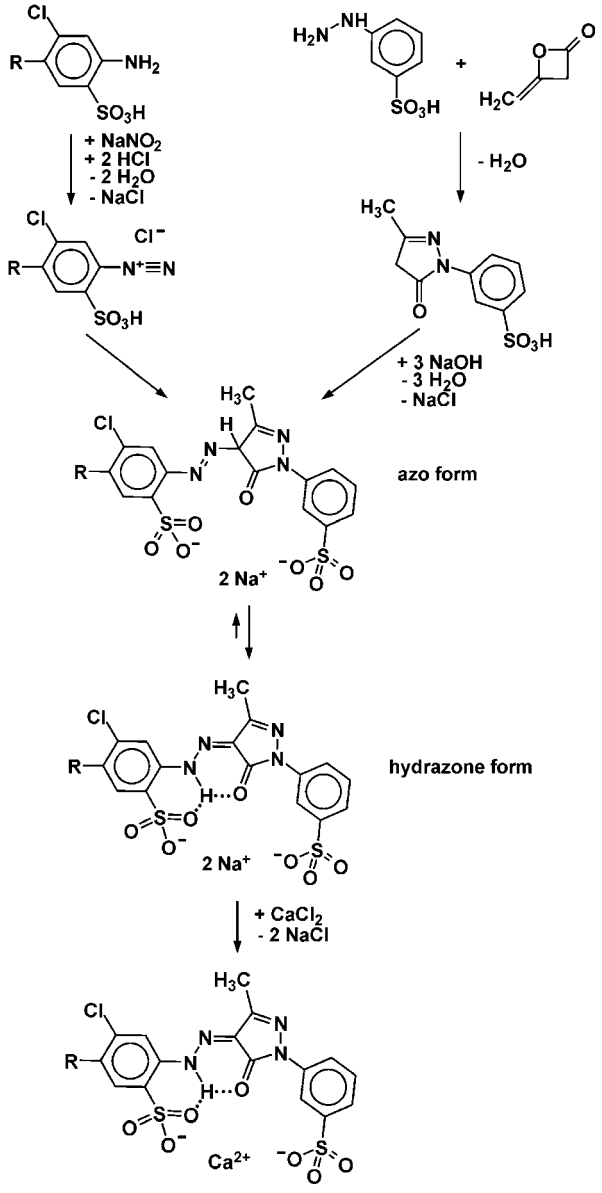

Figure 2
Industrial synthesis of P.Y. 183 (R = Cl) and P.Y. 191 (R = CH_3).

Table 1
Summary of the crystal structures reported in this paper.

DMF = *N*,*N*-dimethylformamide; DMAc = *N*,*N*-dimethylacetamide.

Pigment	Phase	Structure solution
P.Y. 183	α (commercial phase)	Powder
	β (commercial phase)	Single crystal
	DMF solvate	Single crystal
	DMAc solvate	Single crystal
P.Y. 191	α (commercial phase)	Powder
	β (commercial phase)	Powder
	DMF solvate	Single crystal

The last synthetic step is the treatment of the sodium salt with $CaCl_2$ to obtain the calcium salt. This procedure is called 'laking'. Laked pigments are 'azo' compounds containing sulfonate or carboxy groups with a divalent metal counterion (Ca^{2+}, Sr^{2+}, Ba^{2+}, Mn^{2+}).

Laked pigments are industrially produced in quantities of $\sim$ 60 000 tons per year and with an annual sales volume of more than 200 Mio Euro. Although laked pigments have been known for more than 100 years (N.N., 1902), no crystal structure of any industrial laked pigment has been published until now; only the crystal structure of a non-commercial dichloro derivative of Pigment Red 57 was determined from single-crystal data (Kennedy *et al.*, 2000*a*,*b*). For yellow laked pigments no crystal structures have been elucidated at all. The reason lies in the very low solubility of the pigments in all solvents, impeding the growth of single crystals suitable for X-ray analysis.

In our attempts to grow single crystals of P.Y. 191 and P.Y. 183 we performed extensive recrystallizations in many solvents and over a wide range of temperatures. The only single crystals we could obtain were β-P.Y. 183 and three solvates (see Table 1). Hence, the crystal structures of α-P.Y. 183, α-P.Y. 191 and β-P.Y. 191 (which is not isostructural with β-P.Y. 183) were determined from X-ray powder data.

For reference, the crystal structures reported in this paper are summarized in Table 1. Atomic coordinates are available in the supplementary material.[1]

The structure solutions from powder data were complicated by two factors:

(i) The exact number of water molecules was not known.

(ii) From the crystal symmetries ($P\bar{1}$, Z = 2) it was obvious that the asymmetric unit contains one organic anion in a general position; but it was unknown if the Ca counterion is also in a general position or if there are two symmetrically independent Ca ions on special positions (inversion centres).

These difficulties were overcome by using a combination of direct-space methods and Rietveld refinement for structure solution. This combination was made easier by the recently developed link between the programs *DASH* (David *et al.*,

[1] Supplementary data for this paper are available from the IUCr electronic archives (Reference: OG5036). Services for accessing these data are described at the back of the journal.

2006) and *TOPAS* (Coelho, 2007), which automatically generates the input files for *TOPAS*, including restraints on the molecular geometry.

2. Experimental

2.1. Synthesis and recrystallization

2.1.1. α-P.Y. 183. α-P.Y. 183 is industrially produced. In order to improve the crystallinity a sample of commercial α-P.Y. 183 (Paliotol® Yellow K2270 from BASF) was heated as a suspension in a water/isobutanol mixture under reflux for 1 h. The α phase was obtained as a fine yellow powder with enhanced crystallinity.

2.1.2. β-P.Y. 183. The sodium salt of P.Y. 183 was prepared in analogy to the preparation given for P.Y. 191 using 2-amino-4,5-dichlorobenzene-1-sulfonic acid as a starting material. After completion of the coupling reaction, the mixture was kept at 358 K for 30 min and the yellow solid collected by filtration, washed with water and dried. The resulting sodium salt of P.Y. 183 was obtained in a yield of approximately 98%.

5 g of the sodium salt of P.Y. 183 was dissolved in a mixture of 750 ml *N*-methylpyrrolidone (NMP) and 750 ml of water at 373 K. While maintaining the temperature at 373 K, a solution of 5 g $CaCl_2$ in 200 ml water was added over a period of 2 h. The mixture was cooled to 296 K without stirring and the resulting product was collected by filtration, washed with 100 ml of cold water followed by 100 ml of EtOH, and dried in a vacuum oven at 323 K. The isolated yield was 1.4 g P.Y. 183. The elemental analysis of the product showed 6.5% Ca and 0.12% Na, which confirmed that the laking procedure was successful (calculated: 6.69% Ca, 0% Na).

2.1.3. α-P.Y. 191. α-P.Y. 191 was synthesized with 221 kg of 2-amino-4-chloro-5-methylbenzene-1-sulfonic acid, 254 kg of 1-(3′-sulfophenyl)-3-methyl-5-pyrazolone and 250 kg of calcium chloride, as described by Deucker (1990).

To improve the crystallinity, 5 g of the obtained product was suspended in 100 ml of glycerol and heated as a suspension to 453 K for 15 min. The product was a fine yellow powder of α-P.Y. 191 with enhanced crystallinity.

2.1.4. β-P.Y. 191. 25 g of the α phase of P.Y. 191 was dissolved in 1 L of NMP at 453 K. The mixture was cooled to room temperature and subsequently water was added to force crystallization. The β phase was obtained as a yellow powder (Schmidt *et al.*, 2002*b*).

2.1.5. Solvates. In a beaker ∼0.14 g of P.Y. 183 was dissolved in 1.5 ml of *N*,*N*-dimethylformamide (DMF) by heating. The solution was subsequently cooled to room temperature. The beaker was sealed and the solution was kept for crystallization. After 2 to 4 h yellow crystals of the DMF solvate fell out.

Analogously, single crystals of the *N*,*N*-dimethylacetamide (DMAc) solvate of P.Y. 183 and of the DMF solvate of P.Y. 191 were prepared.

2.2. X-ray powder diffraction

Powders of all phases (except the solvates) were measured on a STOE Stadi-P diffractometer with Cu $K\alpha_1$ radiation [curved Ge(111) primary monochromator; λ = 1.5406 Å] in transmission geometry using a linear position-sensitive detector. The samples were prepared between two Mylar® (polyacetate) films. For data acquisition the STOE software *WinX*^{POW} (STOE & Cie, 2004) was used.

Measurements were made in the range between 2 and 34° in 2θ with steps of 0.02° in 2θ. These data turned out to be fully sufficient for indexing and structure solution. α-P.Y. 191 was additionally measured in a capillary on the same diffractometer in the range between 2 and 70° in 2θ. The powder pattern of β-P.Y. 191 was additionally recorded with synchrotron radiation at the National Synchrotron Light Source at Brookhaven National Laboratory in New York (λ = 0.64982 Å) in the range between 1.0 and 20.9° in 2θ with steps of 0.003° in 2θ.

2.3. Thermal analyses

The thermal analyses (DTA/TG) were performed on a SETARAM TGA 92. Samples of ∼10–20 mg were filled in small corundum crucibles and heated at 3 K min^{-1} to 673 K under a nitrogen atmosphere.

For DSC measurements, a DSC 131 (SETARAM) was used. Samples of ∼5–15 mg were weighed and heated in small closed aluminium crucibles at 3 K min^{-1} to 673 K under a nitrogen atmosphere.

3. Structure determination from powder data (α-P.Y. 183, α-P.Y. 191, β-P.Y. 191)

3.1. Indexing

Accurate peak positions for indexing the powder diagrams of α-P.Y. 183, α-P.Y. 191 and β-P.Y. 191 were obtained by fitting 20 manually selected peaks with an asymmetry-corrected Voigt function (Toraya, 1986) using *DASH*. All patterns could be indexed unambiguously with triclinic unit cells by the program *DICVOL91* (Boultif & Louër, 1991). The indices of reliability *M*(*N*) (de Wolff, 1968) and *F*(*N*) (Smith & Snyder, 1979) were used for the characterization of the quality of indexing. Subsequently full pattern decompositions were carried out with the program *DASH* using the Pawley method (Pawley, 1981).

3.2. Structure solution

From the X-ray powder patterns and the indexing, it was obvious that the crystal structures of the two α-phases are isostructural. Therefore, we performed the crystal structure solution step only on one of the α phases (α-P.Y. 183), and used the result also for the Rietveld refinement of the other α phase (α-P.Y. 191). The powder pattern of β-P.Y. 191 showed significant differences to the pattern of β-P.Y. 183, thus the crystal structure of β-P.Y. 191 also had to be solved from scratch.

For structure solution, the powder patterns were truncated to a real space resolution of 2.7 Å for α-P.Y. 183 (which for Cu $K\alpha_1$ radiation corresponds to 33° 2θ) and of 3.2 Å for β-P.Y. 191 (which for Cu $K\alpha_1$ radiation corresponds to 28° 2θ).

The background was subtracted with a Bayesian high-pass filter (David & Sivia, 2001). Pawley refinement was used to extract integrated intensities and their correlations.

The crystal structures were solved in direct space with the programs *DASH* and *TOPAS* using a combination of simulated annealing (SA) and Rietveld refinement.

The starting molecular geometries of the organic anions were taken from the previously determined single-crystal structures of the DMF and DMAc solvates. The organic anions have five flexible torsion angles (see Fig. 3), which combined with three translational and three orientational degrees of freedom correspond to 11 degrees of freedom.

The X-ray scattering power of a H atom is very low, therefore all water molecules were represented by single O atoms; this reduces the number of degrees of freedom for a water molecule from six to just three. The content of an asymmetric unit with one organic anion, a calcium cation and two water molecules corresponds to a total of 20 degrees of freedom. For the values of the torsion angles τ_1 to τ_5, the conjugated nature of the double and aromatic bonds yields sharp distributions of possible torsion angle values based on single-crystal data from the Cambridge Structural Database (CSD; Allen, 2002). *DASH* allows these sharp distributions to be exploited by restricting the torsion angle to intervals of non-negligible probability, thereby reducing the search space. The resulting intervals are given in Table 2. In the *DASH* runs, the number of SA runs was increased from 10 (default value) to 50 in order to obtain better statistics regarding reproducibility.

3.2.1. α-P.Y. 183. A first approximation to the crystal structure of α-P.Y. 183 was obtained by *DASH* using a model containing an organic moiety and a calcium ion. With this model, a profile χ^2 of 51 was reached.

In order to test if the structure contains a water molecule, a grid search (Chernyshev & Schenk, 1998) was performed with the program *MRIA* (Zlokazov & Chernyshev, 1992). The calculations were carried out with an organic anion and a calcium cation fixed in the positions found during the simulated annealing with *DASH*. The grid search was only carried out for an O atom (*i.e.* a water molecule) using the whole volume of the unit cell with a step width of 0.1 Å. The additional O atom was found to be close to an inversion centre $(0,\frac{1}{2},\frac{1}{2})$. The profile χ^2 is 18.2. The oxygen position was confirmed by *DASH*.

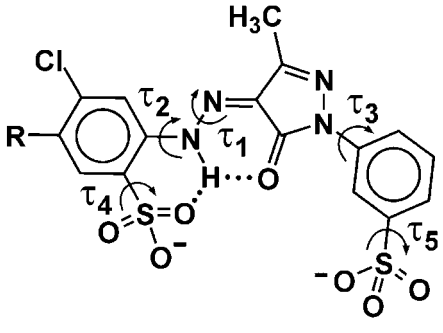

Figure 3
The five flexible torsion angles in the organic anion used in the structure solution step.

Table 2
Allowed ranges for the five flexible torsion angles (°) in the structure solution step.

τ_1	Unimodal	160 to 200
τ_2	Unimodal	160 to 200
τ_3	Bimodal	−45 to +45 and 135 to 225°
τ_4	Free	0 to 360
τ_5	Free	0 to 360

An O atom has eight electrons; hence two O atoms approaching an inversion centre have nearly the same scattering power as a Ca^{2+} ion (18 electrons) situated on the inversion centre itself. This indicated that the Ca^{2+} is not situated on a general position, but on an inversion centre [$(0,\frac{1}{2},\frac{1}{2})$, Wyckoff position 1*g*]. Hence there must be a second, symmetrically independent Ca^{2+} ion, which has to be situated on another inversion centre (there are no other special positions in $P\bar{1}$), *i.e.* on Wyckoff positions 1*a*–1*f* or 1*h*. From the structure it was obvious that the second Ca^{2+} ion has to be placed at $(\frac{1}{2},0,\frac{1}{2})$.

This result was verified by a *DASH* calculation with one organic anion, two Ca^{2+} ions fixed on the inversion centres, and one O atom in a general position. The organic fragment was not kept fixed during this calculation. The O atom moved to a chemically sensible position, and the profile χ^2 dropped to 16.4. All attempts to add a second water molecule led to chemically unreasonable results.

3.2.2. β-P.Y. 191. For β-P.Y. 191, volume considerations suggested the presence of at least two water molecules per asymmetric unit. Structure solutions with one organic moiety, one calcium ion and two O atoms (= two water molecules) per asymmetric unit were tried using the programs *DASH* and *MRIA*. Several solutions yielded the same positions and orientations for the organic fragments, clearly showing layers of alternating polar and non-polar parts, with a clear gap in the polar layer indicating where the Ca atoms and the water molecules should be. However, the positions of Ca^{2+} and the O atoms behaved erratically. This suggested that the Ca atom might not be situated on the general position, but on two special positions (on inversion centres), *i.e.* that the asymmetric unit contained two Ca atoms each with occupancy $\frac{1}{2}$. We therefore tried *DASH* in a model containing one organic fragment, two half-occupied Ca^{2+} ions and two O atoms. The positions of the Ca^{2+} ions were not fixed on inversion centres. The χ^2 values of the solutions did indeed drop, but the two half Ca^{2+} ions did not occupy special positions, and the Rietveld refinement did not progress smoothly; furthermore the calcium coordination was not chemically reasonable.

The problem was solved by means of Rietveld refinement of the partially finished structure. Realising that a half-occupied Ca^{2+} ion has approximately the same scattering power as a

Table 3
Structural parameters of the Rietveld refinements of the three structures determined from powder diffraction data.

	α-P.Y. 183	α-P.Y. 191	β-P.Y. 191
Crystal data			
Chemical formula	$Ca(C_{16}H_{10}Cl_2N_4O_7S_2)\cdot H_2O$	$Ca(C_{17}H_{13}ClN_4O_7S_2)\cdot H_2O$	$Ca(C_{17}H_{13}ClN_4O_7S_2)\cdot 3H_2O$
M_r	563.42	543.0	579.03
Crystal system, space group	Triclinic, $P\bar{1}$	Triclinic, $P\bar{1}$	Triclinic, $P\bar{1}$
Temperature (K)	293	293	293
a, b, c (Å)	5.6894 (3), 10.5943 (6), 18.526 (1)	5.6915 (2), 10.6053 (3), 18.5569 (6)	6.0140 (1), 10.8169 (2), 18.0938 (3)
α, β, γ (°)	73.316 (5), 87.842 (3), 76.127 (3)	72.828 (2), 88.271 (2), 76.423 (1)	85.677 (1), 86.392 (1), 75.783 (1)
V (Å^3)	1037.8 (1)	1039.37 (5)	1136.55 (3)
Z	2	2	2
Radiation type	Cu $K\alpha_1$	Cu $K\alpha_1$	Synchrotron
Wavelength of incident radiation (Å)	1.54056	1.54056	0.649819
μ (mm^{-1})	7.38	6.19	0.518
Specimen shape, size (mm)	Flat sheet, 10 × 1.2	Cylinder, 10 × 0.7	Cylinder, 10 × 0.7
Data collection			
Diffractometer	STOE-Stadi-P	STOE-Stadi-P	NSLS Brookhaven
Specimen mounting	Flat sample holder	Glass capillary	Glass capillary
Scan method	Step	Step	Step
Data-collection mode	Transmission	Transmission	Transmission
2θ values (°)	$2\theta_{min}$ = 3.00, $2\theta_{max}$ = 34.00, $2\theta_{step}$ = 0.02	$2\theta_{min}$ = 2.00, $2\theta_{max}$ = 70.00, $2\theta_{step}$ = 0.01	$2\theta_{min}$ = 1.000, $2\theta_{max}$ = 20.896, $2\theta_{step}$ = 0.003
Refinement			
R_p, R_{wp}, R_{exp}, χ^2	0.061, 0.071, 0.068, 1.08	0.091, 0.100, 0.055, 3.39	0.099, 0.206, 0.206, 0.35
Excluded region(s)	None	None	None
No. of data points	1550	6800	6633
No. of parameters	181	187	207
H-atom treatment	Calculated	Calculated	Calculated
No. of restraints	117	126	126

water molecule, it seemed likely that the O atoms and the half-occupied Ca^{2+} ions had to be interchanged. Therefore, all O atoms (8 electrons) and all half-occupied Ca^{2+} ions ($\frac{1}{2} \times 18 = 9$ electrons) were set to fluorine atoms (9 electrons) and their occupancies were allowed to refine freely using the program *TOPAS*. This led to a smooth and stable Rietveld refinement with occupancies of 2.1, 1.0, 0.8 and 0.8, corresponding to 18.9, 9.0, 7.2 and 7.2 electrons, respectively. None of the F atoms was close to a special position. From the occupancies, one calcium ion and three water molecules could readily be identified. Hence the structure should contain not two, but three water molecules.

Replacing the four F atoms with one calcium ion and three O atoms with full occupancies led to a stable Rietveld refinement with a chemically plausible calcium coordination.

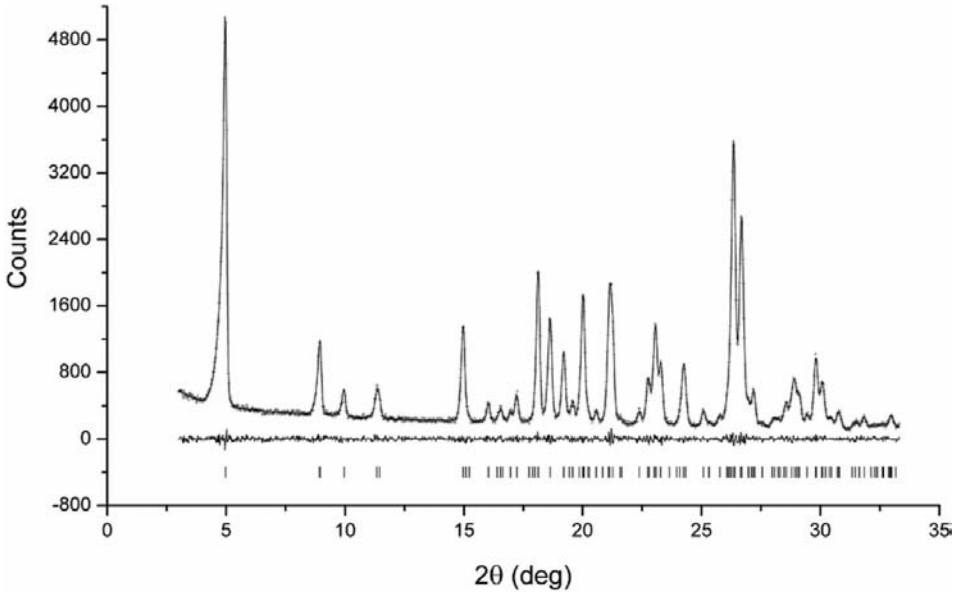

Figure 4
Rietveld plot of α-P.Y. 183. The experimental data points are shown as crosses, the calculated pattern as a solid line and the difference curve as a line under the profiles. Tick marks are shown as vertical dashes.

3.3. Final Rietveld refinement

Rietveld refinements of α-P.Y. 183, α-P.Y. 191 and β-P.Y. 191 were carried out with *TOPAS* using all diffraction data, without restricting the 2θ ranges. For β-P.Y. 191, synchrotron data were used. The *TOPAS* input file was generated automatically by the *DASH*-to-*TOPAS* link available in *DASH*. Suitable chemical restraints were automatically generated by *DASH* for all bond lengths, valence angles and the planarity of the aromatic

ring systems. Anisotropic peak broadening was included to allow the peak profiles to be described accurately. A preferred orientation correction was not necessary. The global isotropic temperature factor was allowed to refine, with the isotropic temperature factors of the H atoms being constrained at 1.2 times the value for the C, N, O and S atoms. For the Cl atoms isotropic displacement factors were refined individually. All Rietveld refinements converged with good R values and smooth difference curves (Table 3; Figs. 4–6).

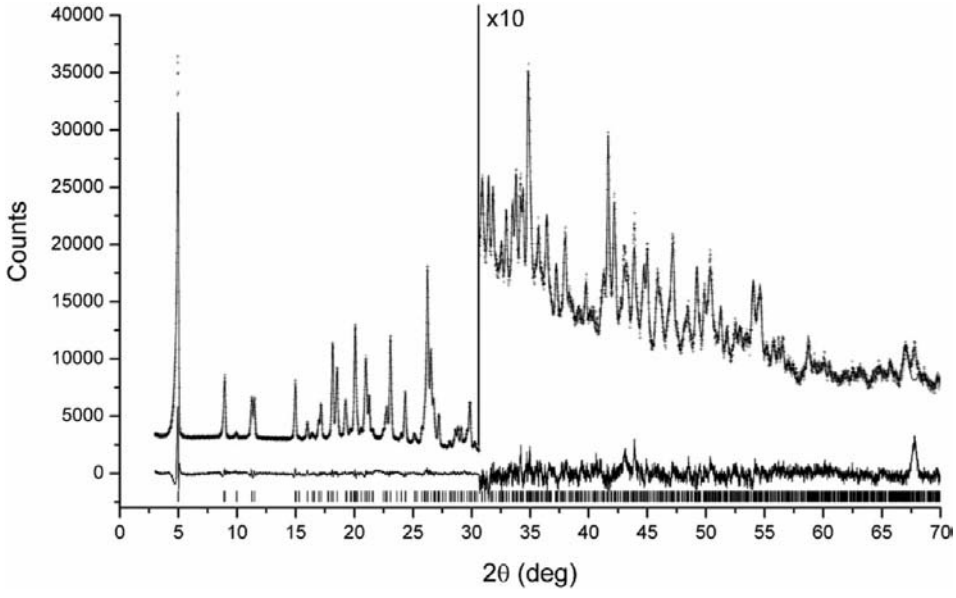

Figure 5
Rietveld plot of α-P.Y. 191. The experimental data points are shown as crosses, the calculated pattern as a solid line and the difference curve as a line under the profiles. Tick marks are shown as vertical dashes (laboratory data). The peak at 67.8° is known from experience to stem from the experimental set up.

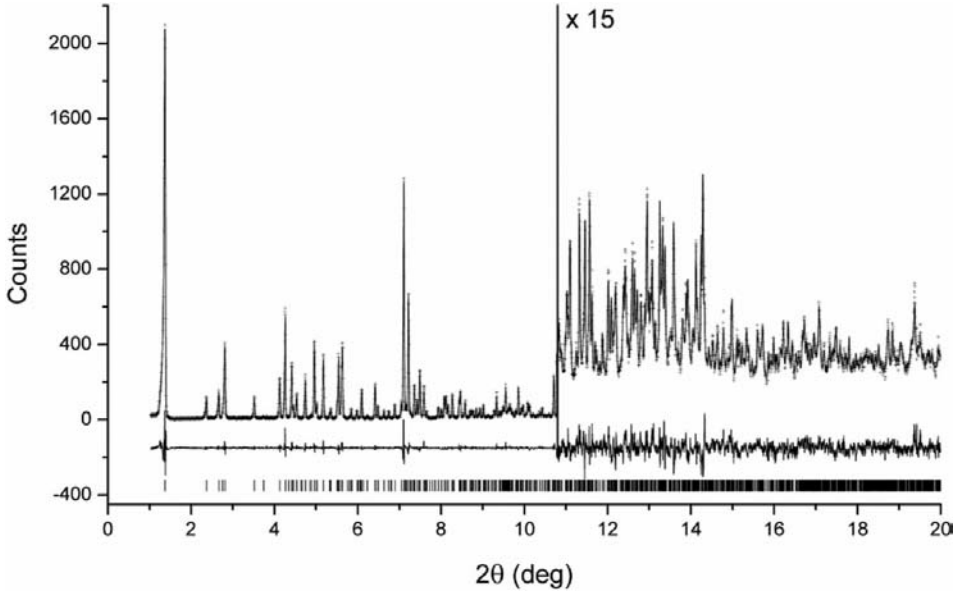

Figure 6
Rietveld plot of β-P.Y. 191. The experimental data points are shown as crosses, the calculated pattern as a solid line and the difference curve as a line under the profiles. Tick marks are shown as vertical dashes (synchrotron data, λ = 0.64982 Å).

3.3.1. α-P.Y. 183. H atoms for water molecules were added in calculated positions using the program *MERCURY* 2.0, according to close O···O contacts indicating the presence of hydrogen bonds. Afterwards a Rietveld refinement was performed again (Fig. 4).

3.3.2. α-P.Y. 191. α-P.Y. 191 and α-P.Y. 183 are isostructural. Since the structure of α-P.Y. 183 had been solved from powder diffraction data, for α-P.Y. 191 only a Rietveld refinement was carried out, starting from the coordinates of the α-P.Y. 183 structure. To change from P.Y. 183 to P.Y. 191, one of the Cl atoms of P.Y. 183 was replaced by a CH_3 group using the program *Cerius*[2] (Accelrys, 2003). The Rietveld plot is shown in Fig. 5.

3.3.3. β-P.Y. 191. A preliminary Rietveld refinement had already been carried out during the structure solution of β-P.Y. 191 from laboratory data (see §3.2.2). In this stage the water molecules were represented only by O atoms. Subsequently the positions of the H atoms of the three water molecules were calculated using the DREIDING 2.21 force-field within the program package *Cerius*[2]. During this optimization the coordinates of all other atoms, as well as the lattice parameters were fixed.

The structure was Rietveld-refined using synchrotron data. The difference curve is almost a straight line (Fig. 6).

3.4. Thermal analyses

The α phases of P.Y. 183 and P.Y. 191 are monohydrates; nevertheless, they are remarkably stable. α-P.Y. 183 as well as α-P.Y. 191 can be extruded in polyethylene at 573 K without any colour change (Herbst & Hunger, 2004). As is visible from the thermogravimetrical analyses, both α phases remain unchanged until $\sim$ 523 K, whereas at temperatures of *ca* 533 to 573 K they slowly release water. After heating α-P.Y. 183 to 673 K with subsequent cooling to room temperature the X-ray powder diagram reveals the presence of the α phase (which indicates that the dehydration is reversible).

Table 4
Structural parameters and figures-of-merit of the refinements of the structures determined from single-crystal data.

Chemical composition	β-P.Y. 183 P.Y. 183·3H_2O	Solvates		
		P.Y. 183·3DMF	P.Y. 183·4DMAc	P.Y. 191·4DMF
Crystal data				
Chemical formula	$Ca(C_{16}H_{10}Cl_2N_4O_7S_2)\cdot 3H_2O$	$Ca(C_{16}H_{10}Cl_2N_4O_7S_2)\cdot 3C_3H_7NO$	$C(C_{16}H_{10}Cl_2N_4O_7S_2)\cdot 4C_4H_9NO$	$Ca(C_{17}H_{13}ClN_4O_7S_2)\cdot 4C_3H_7NO$
M_r	599.43	764.67	893.87	817.35
Crystal system, space group	Triclinic, $P\bar{1}$	Triclinic, $P\bar{1}$	Monoclinic, $P2_1/c$	Triclinic, $P\bar{1}$
Temperature (K)	203	100	100	100
a, b, c (Å)	5.574 (3), 10.925 (3), 18.801 (5)	10.5951 (10), 11.4600 (11), 15.2829 (15)	8.9032 (9), 26.283 (4), 17.7857 (18)	8.1479 (5), 13.1042 (8), 18.1233 (12)
α, β, γ (°)	98.605 (19), 92.35 (3), 102.77 (3)	82.876 (8), 70.639 (8), 70.015 (7)	90, 93.887 (8), 90	90.134 (5), 99.765 (5), 104.181 (5)
V (Å^3)	1100.8 (8)	1645.2 (3)	4152.3 (9)	1847.0 (2)
Z	2	2	4	2
Radiation type	Cu $K\alpha$	Mo $K\alpha_1$	Mo $K\alpha_1$	Mo $K\alpha_1$
μ (mm^{-1})	7.09	0.55	0.45	0.42
Specimen shape, size	Needle, 0.40 × 0.02 × 0.02	Block, 0.34 × 0.24 × 0.15	Plate, 0.46 × 0.20 × 0.05	Block, 0.43 × 0.41 × 0.37
Data collection				
Diffractometer	Siemens P4	STOE IPDS II two-circle	STOE IPDS II two-circle	STOE IPDS II two-circle
Data collection method	$\theta/2\theta$ scan	ω scan	ω scan	ω scan
Absorption correction	*DIFABS* Empirical (*SHELXA*)	Multi-scan†	Multi-scan†	Multi-scan†
T_{min}	0.414	0.837	0.821	0.839
T_{max}	1.000	0.923	0.978	0.859
No. of measured, independent and observed reflections	3144, 2790, 1925	18 279, 7067, 4933	23 644, 7640, 4542	37 376, 8457, 6914
Criterion for observed reflections	$I > 2\sigma(I)$	$I > 2\sigma(I)$	$I > 2\sigma(I)$	$I > 2\sigma(I)$
R_{int}	0.073	0.042	0.078	0.043
θ_{max} (°)	55.4	27.6	26.1	27.6
Refinement				
Refinement on	F^2	F^2	F^2	F^2
$R[F^2 > 2\sigma(F^2)]$, $wR(F^2)$, S	0.055, 0.143, 1.02	0.026, 0.054, 0.80	0.078, 0.211, 1.02	0.028, 0.077, 0.97
No. of reflections	2790	7067	7640	8457
No. of parameters	347	435	522	482
H-atom treatment	Mixture‡	Mixture‡	Mixture‡	Constrained
$(\Delta/\sigma)_{max}$	0.002	0.001	< 0.0001	0.001
$\Delta\rho_{max}$, $\Delta\rho_{min}$ (e Å^{-3})	0.55, −0.47	0.29, −0.32	1.31, −0.67	0.48, −0.40
Extinction method	*SHELXL*	None	None	None
Extinction coefficient	0.0004 (3)	–	–	–

† Based on symmetry-related measurements. ‡ Mixture of independent and constrained refinement.

Temperature-dependent X-ray diffraction analysis of α-P.Y. 191 shows that in an open capillary at 523 K the compound transforms to a new phase; further heating to 573 K results in a second new phase. After cooling back to room temperature and waiting for 2 d, the α phase formed again. The crystallinity of the new phases was not sufficient to determine their crystal structures. Heating α-P.Y. 191 to 673 K with subsequent cooling to room temperature leads to a dull yellow powder of low crystallinity, which according to the X-ray powder diagram may be a nanocrystalline α phase.

The anhydrous phases of P.Y. 183 and P.Y. 191 could, in principle be used as pigments, too; but they are not produced industrially since the heat stability of the well established products α-P.Y. 183 and α-P.Y. 191 fulfils all technical requirements.

The β phases are less stable than the α phases: combined powder diffraction and thermogravimetrical analyses of β-P.Y. 183 and β-P.Y. 191 show that, upon heating, the β phases slowly release water and transform to the α phases, which above 523 K lose further water. In total, three water molecules are released.

4. Single-crystal structure analyses

4.1. β-P.Y. 183

A thin, orange needle of β-P.Y. 183 with a diameter of *ca* 20 µm and a length of *ca* 400 µm was measured on a Siemens P4 diffractometer, equipped with a fine-focus sealed tube and a graphite monochromator, using Cu $K\alpha$ radiation (λ = 1.54178 Å). An empirical absorption correction was carried out by *SHELXL* (Sheldrick, 2008). The crystal structure was solved by direct methods and completed by difference-Fourier methods using the *SHELXS*97 package (Sheldrick, 2008). The structure was refined by full-matrix least-squares on F^2 using all reflections (*SHELXL*97; Sheldrick, 2008). All non-H atoms

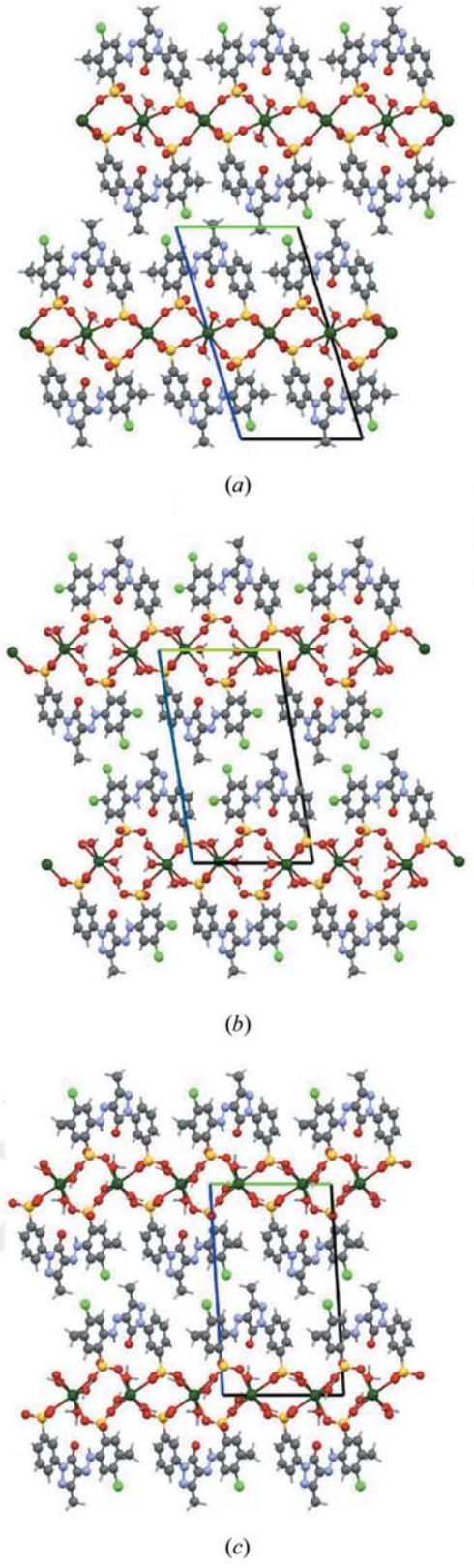

Figure 7
The crystal structures of (*a*) α-P.Y. 191, (*b*) β-P.Y. 183 and (*c*) β-P.Y. 191. For (*a*), (*b*) and (*c*): view direction [100], **b** axes horizontal, **c** axes vertical. Colour codes: Ca atoms green, O red, S yellow, C dark grey, N blue, Cl light green balls, H grey sticks. All crystal structure drawings were made with *Mercury* 2.0 (Macrae *et al.*, 2008). This figure is in colour in the electronic version of this paper.

were refined anisotropically. H atoms bonded to carbon and nitrogen were refined using a riding model with N—H distances of 0.87 Å, and C—H distances of 0.94 Å for aromatic and 0.97 Å for aliphatic C atoms. Methyl groups were treated as rotating fragments. The positions of the H atoms of the three water molecules were refined with constraints on the O—H distances (0.83 Å) and H—O—H angles (105°). Crystallographic data are given in Table 4.

4.2. Solvates

X-ray diffraction measurements were carried out on a STOE IPDS-II two-circle single-crystal diffractometer (STOE & Cie, 2001) using graphite-monochromated Mo $K\alpha_1$ radiation (λ = 0.71073 Å) and equipped with an image-plate detector. An absorption correction was carried out using the *MULABS* (Blessing, 1995) option in *PLATON* (Spek, 2003).

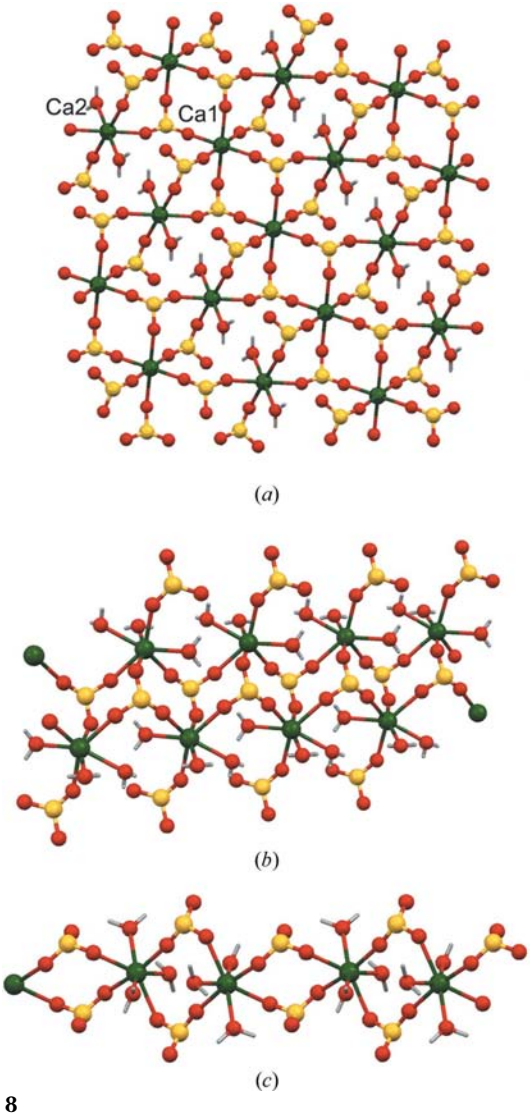

Figure 8
Calcium sulfonate networks in P.Y. 183 and P.Y. 191: (*a*) two-dimensional network in the crystal structures of α-P.Y. 183 and α-P.Y. 191; (*b*) double chain along the **a** axis in β-P.Y. 183; (*c*) chain along the **b** axis in β-P.Y. 191. This figure is in colour in the electronic version of this paper.

Table 5
Ca—O distances (Å) in the structures of the α and β phases.

O atoms from water molecules are indicated by 'w'.

Atoms	α-P.Y. 183	α-P.Y. 191
Ca1—O30	2.29 (2)	2.31 (1)
Ca1—O39	2.33 (2)	2.28 (1)
Ca1—O40	2.35 (2)	2.41 (1)
Ca2—O28	2.27 (2)	2.32 (1)
Ca2—O38	2.31 (2)	2.34 (1)
Ca2—O44^{w}	2.27 (2)	2.44 (1)
Mean	2.30 (3)	2.35 (6)

Mean value from CSD for Ca—O in [CaO_6]: 2.34 (7)

Atoms	β-P.Y. 183	Atoms	β-P.Y. 191
Ca—O7	2.404 (5)	Ca—O29	2.32 (1)
Ca—O25	2.388 (4)	Ca—O30	2.49 (1)
Ca—O26	2.405 (5)	Ca—O38	2.32 (1)
Ca—O27	2.385 (5)	Ca—O40	2.46 (1)
Ca—O30^{w}	2.390 (5)	Ca—O46^{w}	2.38 (1)
Ca—O31^{w}	2.408 (5)	Ca—O47^{w}	2.43 (1)
Ca—O32^{w}	2.460 (6)	Ca—O48^{w}	2.44 (1)
Mean	2.41 (2)		2.41 (6)

Mean value from CSD for Ca—O in [CaO_7]: 2.45 (11)

The intensities of the reflections were corrected for Lorentz and polarization effects. The crystal structures were solved by direct methods (Sheldrick, 2008) and refined by full-matrix least-squares using the *SHELXL*97 program (Sheldrick, 2008). All H atoms were located in difference-Fourier maps and then treated as riding atoms, with C—H bond lengths in the range 0.95–0.98 Å and N—H distance of 0.88 Å. For methyl atoms, $U(H) = 1.5U_{eq}(C)$ was used, while for other H atoms, $U(H) = 1.2U_{eq}(C, N)$. The methyl groups were allowed to rotate but not to tip. The NH atoms in P.Y. 183·3DMF and P.Y. 183·4DMAc were freely refined.

Crystallographic data are included in Table 4. The reason for the slightly increased wR_2 of P.Y. 183·4DMAc might be that the DMAc molecules show increased thermal motion and have slightly enlarged anisotropic displacement parameters. Nevertheless, the quality of the data allowed for free refinement of the amino H atom.

5. Discussion of the crystal structures

5.1. α-P.Y. 183 and α-P.Y. 191

The α phases of P.Y. 183 and P.Y. 191 are isostructural and both are monohydrates. The structure of α-P.Y. 191 is displayed in Fig. 7(*a*). The asymmetric unit contains one organic anion, two symmetrically independent calcium cations on inversion centres, and one water molecule. Both Ca^{2+} ions are octahedrally coordinated, each by six O atoms: Ca1 is connected with four O atoms from sulfonate groups and with two O atoms from water molecules; Ca2 is connected with six O atoms from the sulfonate groups.

The sulfonate groups and calcium ions build a two-dimensional network (see Fig. 8*a*). The Ca···O distances in the α phases are in very good agreement with those present in sixfold oxygen-coordinated calcium in the CSD (see Table 5).

The α phases form double-layer structures. The non-polar layers consist of the organic moieties; the polar layers contain the sulfonate groups, the calcium ions and the water molecules. The polar layer is held together by Coulomb interactions and hydrogen bonds, whereas in the non-polar layer the molecules are mainly connected by van der Waals interactions (and additional Coulomb interactions).

5.2. β-P.Y. 183 and β-P.Y. 191

β-P.Y. 183 and β-P.Y. 191 are trihydrates: the asymmetric units contain one organic anion, one calcium cation and three water molecules. The Ca^{2+} ions have a sevenfold coordination: they are connected to four O atoms from sulfonate groups and three O atoms from water molecules.

The Ca···O distances vary from 2.32 to 2.49 Å, which is well within the usual range found in the CSD for Ca^{2+} ions surrounded by seven O atoms (see Table 5). The coordination polyhedron is a distorted pentagonal pyramid for both structures.

As in the α phases, the structures consist of polar and non-polar layers, with the polar layer containing Ca^{2+}, SO_3^- and H_2O moieties, and the non-polar layer consisting of the organic framework (Figs. 7*b* and *c*). Within the polar layer the water molecules generate an extensive hydrogen-bond network.

The Ca···O distances in the β-phases are in agreement with those present in sevenfold oxygen-coordinated calcium in the CSD (see Table 5).

Although β-P.Y. 183 and β-P.Y. 191 are both trihydrates, do crystallize in the same space group ($P\bar{1}$, $Z = 2$), are layer structures, and even have the same Ca coordination, their crystal structures are clearly different: in β-P.Y. 191 the sulfonate groups and calcium ions form chains along the **b** axis (Fig. 8*c*), whereas in β-P.Y. 183 the sulfonate groups and calcium ions build double chains along the **a** axis (Fig. 8*b*).

5.3. P.Y. 183·3DMF

The organic anions and calcium cations form double chains in the (001) plane. The Ca^{2+} ion has a sixfold coordination, and is surrounded by three solvent molecules and three O atoms from sulfonate groups of different organic anions.

Every organic anion is connected to three calcium cations: the sulfonate group at the dichlorophenyl ring is connected with one calcium ion, whereas the other sulfonate group is bound to two calcium ions *via* O32 and O33 (Fig. 9*a*).

As in all other structures of P.Y. 183 and P.Y. 191, an intramolecular bifurcated hydrogen bond is formed between the proton of the hydrazone group and the O atoms of the pyrazolone fragment and the sulfonate group neighbouring the hydrazone fragment.

The remaining space between two organic moieties, which are linked by two calcium cations, is filled by two DMF molecules, which coordinate to the calcium cations.

5.4. P.Y. 183·4DMAc

P.Y. 183·4DMAc is a dimer structure consisting of two calcium ions bridged by two sulfonate groups and eight solvent molecules. The calcium ion has sixfold coordination (Fig. 9*b*). Every calcium cation is surrounded by four solvent molecules and two O atoms from sulfonate groups of different organic anions.

The sulfonate group of the phenylpyrazolone moiety is connected to two calcium cations.

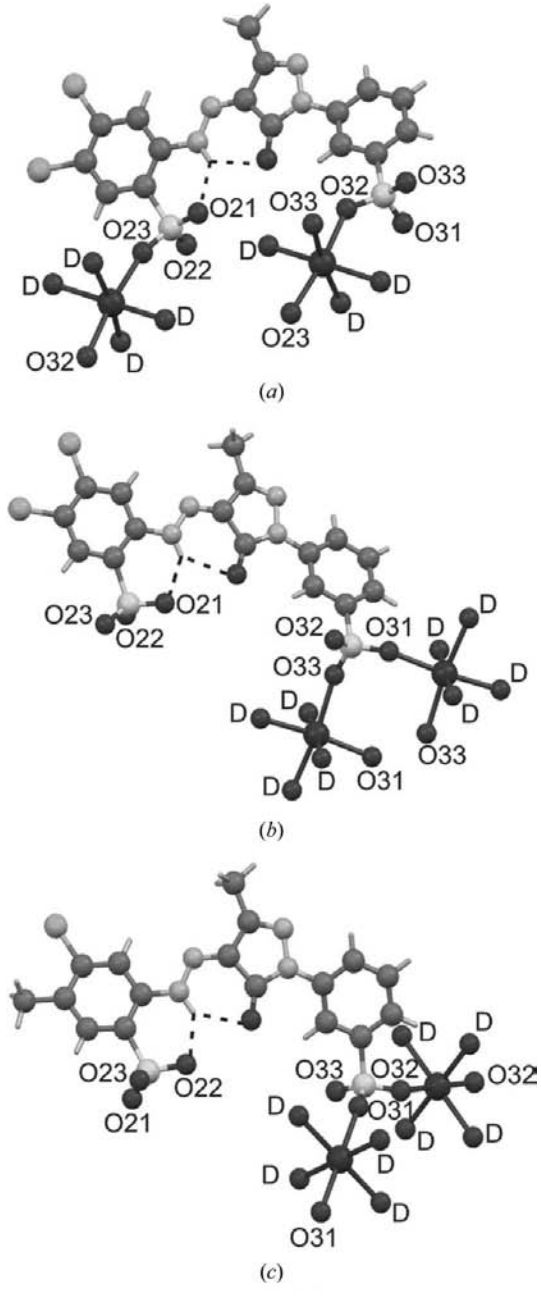

Figure 9
Calcium coordination in the crystal structures of (*a*) P.Y. 183·3DMF, (*b*) P.Y. 183·4DMAc and (*c*) P.Y. 191·4DMF. O atoms of DMF and DMAc molecules are denoted with 'D'.

Surprisingly, the other sulfonate group is not connected to any calcium ion. The shortest distance between the S atom of this sulfonate group and the Ca^{2+} ion is 8.6 Å.

The compound forms a double herringbone packing along the **b** axis.

5.5. P.Y. 191·4DMF

The organic anions and the calcium cations build a chain structure along the **b** axis. The calcium ion is surrounded by the O atoms of four solvent molecules and by two O atoms from sulfonate groups of different organic anions (Fig. 9*c*). As in P.Y. 183·4DMAc every organic anion is connected by two calcium cations *via* one sulfonate group, whereas the other sulfonate group is not involved in any intermolecular bonding.

6. Conclusion

In this article a useful approach for structure solution from powder diffraction data for organic compounds is presented. The coordinates of the large molecular fragments of the crystal structures were found by means of real-space methods with the program *DASH*. The coordinates of the calcium ions and the water molecules were determined by combining real-space methods (*DASH* and *MRIA*) and repeated Rietveld refinements (*TOPAS*) of the partially finished crystal structures. This procedure was used for quite complex structures, *e.g.* β-P.Y. 191 with one flexible molecular anion, one Ca^{2+} cation and three water molecules in the asymmetric unit. The method works even with laboratory powder diffraction data.

All the α and β phases of P.Y. 183 and of P.Y. 191 show similar structures, built from polar and non-polar layers; even the space groups are identical ($P\bar{1}$) and the lattice parameters are quite similar. Nevertheless, only α-P.Y. 183 and α-P.Y. 191 are isostructural. The other crystal structures differ in their Ca^{2+}-sulfonate connection patterns which are a chain for β-P.Y. 191, a double chain for β-P.Y. 183 and a two-dimensional network for α-P.Y. 183 and α-P.Y. 191. In the α phases, as well as in the three solvates, the Ca^{2+} ions are octahedrally coordinated by six O atoms. This coordination geometry is generally preferred for Ca^{2+} ions surrounded by O atoms of organic ligands. In contrast both β phases show a less-frequent sevenfold coordination with O atoms forming a distorted pentagonal bipyramid around the calcium ion.

In the α and β phases as well as in P.Y. 183·3DMF both sulfonate groups are bound to Ca^{2+} ions, as expected. In contrast, in the crystal structures of P.Y. 183·4DMAc and P.Y. 191·4DMF the most remarkable feature is that the Ca^{2+} ion coordinates only to one of the two SO_3^- groups, whereas the other SO_3^- group is not connected to any solvent, water or counter ion, but is surrounded by aliphatic CH and CH_3 groups only. The reason for this electrostatically unfavourable behaviour remains obscure.

Upon heating, the β phases (trihydrates) of P.Y. 183 and P.Y. 191 release water molecules and convert to the α phases (monohydrates), which release their water molecules at temperatures above 523 K. The pigments are organic calcium

sulfonates, and the stepwise release of water is reminiscent of their inorganic counterpart, calcium sulfate: upon heating $CaSO_4{\cdot}2H_2O$ (gypsum) converts to a hemihydrate which releases the final water molecule at 433 K (Holleman, 1906), *i.e.* the dehydration temperature is almost 100 K lower than for α-P.Y. 183 and α-P.Y. 191. This is a rare case where organic crystals are more stable than their inorganic counterparts.

Dr Martin Ermrich (http://www.roentgenlabor-ermrich.de/), Dr Lothar Fink (Goethe University, Frankfurt am Main), Dr Robert Dinnebier (MPI for solid state research, Stuttgart) and Dr Fabia Gozzo (PSI, Villigen) are gratefully acknowledged for the collection of the powder diffraction patterns. The work was done with the financial support of Clariant GmbH and a grant of the Deutscher Akademischer Austauschdienst (DAAD), program 'Forschungsaufenthalte für Hochschullehrer und Wissenschaftler' 2007, for SNI.

References

Accelrys (2003). *Cerius*^{2}, Version 4.9. Accelrys Ltd, Cambridge, England.
Allen, F. H. (2002). *Acta Cryst.* B**58**, 380–388.
Blessing, R. H. (1995). *Acta Cryst.* A**51**, 33–38.
Boultif, A. & Louër, D. (1991). *J. Appl. Cryst.* **24**, 987–993.
Chernyshev, V. V. & Schenk, H. (1998). *Z. Kristallogr.* **213**, 1–3.
Coelho, A. A. (2007). *TOPAS Academic 4.1*, http://members.optusnet.com.au/alancoelho.
David, W. I. F., Shankland, K., van de Streek, J., Pidcock, E., Motherwell, W. D. S. & Cole, J. C. (2006). *J. Appl. Cryst.* **39**, 910–915.
David, W. I. F. & Sivia, D. S. (2001). *J. Appl. Cryst.* **34**, 318–324.
Deucker, W. (1990). European Patent EP 0361431.
Herbst, W. & Hunger, K. (2004). *Industrial Organic Pigments: Production, Properties, Applications*, 3th ed. Weinheim: Wiley-VCH.
Holleman, A. F. (1906). *Lehrbuch der unorganischen [sic!] Chemie*, 4. Auflage, p. 342. Leipzig: Veit and Co.
Kennedy, A. R., McNair, C., Smith, W. E., Chisholm, G. & Teat, S. J. (2000*a*). *Angew. Chem.* **112**, 652–654.
Kennedy, A. R., McNair, C., Smith, W. E., Chisholm, G. & Teat, S. J. (2000*b*). *Angew. Chem. Int. Ed.* **39**, 638–640.
Macrae, C. F., Bruno, I. J., Chisholm, J. A., Edgington, P. R., McCabe, P., Pidcock, E., Rodriguez-Monge, L., Taylor, R., van de Streek, J. & Wood, P. A. (2008). *J. Appl. Cryst.* **41**, 466–470.
N.N. (1902). (Griesheim-Elektron) Deutsches Reichspatent DRP 145908.
Pawley, G. S. (1981). *J. Appl. Cryst.* **14**, 357–361.
Schmidt, M. U. (2008). Unpublished results.
Schmidt, M. U., Acs, A., Jung, R. & Schui, F. (2002*a*). US Patent No. 6602342 B2.
Schmidt, M. U., Acs, A., Jung, R. & Schui, F. (2002*b*). European Patent EP 1170338.
Sheldrick, G. M. (2008). *Acta Cryst.* A**64**, 112–122.
Smith, G. S. & Snyder, R. L. (1979). *J. Appl. Cryst.* **12**, 60–65.
Spek, A. L. (2003). *J. Appl. Cryst.* **36**, 7–13.
STOE & Cie (2004). *WinX*^{POW}. STOE & Cie, Darmstadt, Germany.
STOE & Cie (2001). *X-Area*, Version 2.0. STOE & Cie, Darmstadt, Germany.
Toraya, H. (1986). *J. Appl. Cryst.* **19**, 440–447.
Wolff, P. M. de (1968). *J. Appl. Cryst.* **1**, 108–113.
Zlokazov, V. B. & Chernyshev, V. V. (1992). *J. Appl. Cryst.* **25**, 447–451.